OXYGEN ISOTOPE ANALYSIS OF FINE-GRAINED COMETARY MATERIAL FROM THE BULB OF A STARDUST TRACK R. C. Ogliore[1], G. R. Huss[1], K. Nagashima[1], A. J. Westphal[2], [1]Hawai'i Institute of Geophysics and Planetology, University of Hawai'i at Mānoa, Honolulu, HI 96822, USA, [2]Space Sciences Laboratory, University of California Berkeley, Berkeley, CA 94720, USA.

Introduction

Cometary material captured in aerogel by the Stardust mission spans a size range from sub-μm dust in the bulbs of type B and C tracks [1] to several-μm particles that tend to be found at or near the track termini. The larger particles from comet Wild 2 are mostly high-temperature objects [2], including CAI and chondrule fragments [3, 4]. The O isotopic composition of a sample of these particles shows similarities to chondrules in CR meteorites [5], with LIME olivines clustering at Δ^{17}O ≈ -23‰ and FeO-rich particles ranging from -1.5‰ to $+2.5$‰.

The fine-grained material in the bulbs of Stardust tracks is not as well-studied due to the condition it is in—dispersed and intimately mixed with melted, insulating aerogel. However, this material likely contains pristine, unprocessed cometary material [6] that is not well represented by the larger Stardust fragments.

Here, we report a technique to measure the O isotopic composition of fine-grained Stardust material in aerogel by SIMS. We present multiple standards to verify the accuracy of our technique, and measurements from the bulb of a type B Stardust track.

Methods

We extracted a 1 mm^2 section from the wall of Stardust track C2052,2,74 for O-isotope measurements. Additionally, we prepared three standards to assess the accuracy of our SIMS O measurements: 1) Powdered terrestrial basalt pressed into aerogel, 2) Olivine powder shot into aerogel at ~6 km/s, 3) Spinel separates from the Allende meteorite pressed into aerogel (having non-TFL composition: δ^{18}O, δ^{17}O = -40‰, -40‰).

With a Teflon-coated anvil and a press, we compressed the aerogel samples into indium. The aerogel porosity was sufficiently reduced to allow a conductive Au coat to be applied. The samples were then mounted under a Au-coated Si_3N_4 window to create a flat, conducting surface for SIMS analysis [7].

Using a <3 pA primary Cs+ beam on the University of Hawaii Cameca ims 1280 ion probe, we acquired 15μm$\times$15μm scanning ion maps for a total of ~15 hours per map. In each ~75s measurement cycle, we collected $^{16}O^-$, $^{17}O^-$, $^{18}O^-$ simultaneously on three electron multipliers and then peak-jumped to $^{28}Si^-$, $^{27}Al^{16}O^-$, $^{24}Mg^{16}O^-$, and $^{56}Fe^{16}O^-$. The mass resolving power for $^{17}O^-$ was ~5500 to minimize the contribution of the $^{16}OH^-$ interference on $^{17}O^-$. We registered the 720 maps using the $^{16}O^-$ map to account for drift during the long measurement, then corrected $^{18}O/^{16}O$ and $^{17}O/^{16}O$ as a power-law function of ^{16}O count rate.

We seek to determine the O composition of the cometary (or standard) material relative to the surrounding aerogel, which has a known O isotopic composition, δ^{18}O≈ -1.1 and δ^{17}O≈ -0.5 [8]. The cometary/standard material contains Mg, Al, or Fe at a much stronger concentration than the aerogel. From our collected Mg, Al, and Fe maps we are easily able to distinguish (using a simple thresholding algorithm, or drawing by eye) contiguous regions of cometary material from aerogel (see Figure 2).

With the cometary material separated from the aerogel, we calculate the $^{18}O/^{16}O$ and $^{17}O/^{16}O$ in individual cometary regions. We normalize this composition to the surrounding aerogel O composition and calculate uncertainties by the following Monte Carlo method. For each region of interest consisting of N cometary pixels, we randomly select N background aerogel pixels and calculate the $^{18}O/^{16}O$ and $^{17}O/^{16}O$ ratios in this set of aerogel pixels. We calculate δ^{18}O and δ^{17}O for the ROI relative to these aerogel ratios, and repeat the process 10^5 times. From this distribution, we compute a mean and standard deviation which correspond to the δ^{18}O and δ^{17}O values and uncertainties for the cometary region.

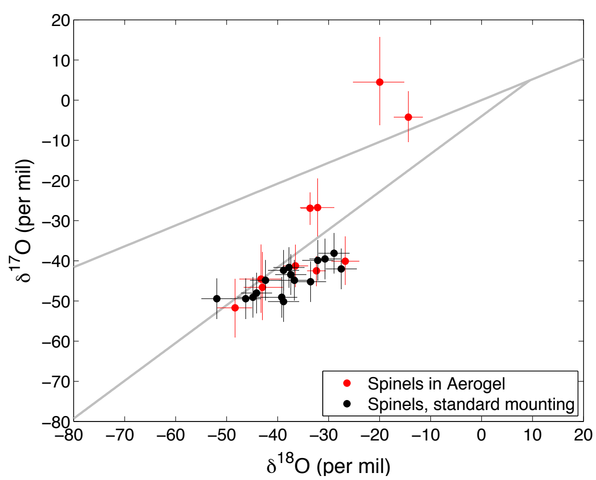

Figure 1: Oxygen 3-isotope plot showing Allende spinel separates pressed into aerogel (red, this study) and individual spinels measured on Au foil (black, [9]). Uncertainties are 2σ. Outliers are likely metamorphosed spinels, chondrule fragments, or contaminants.

Results

We found the powdered basalt pressed into aerogel to have O composition near the TFL. The composition of the olivine shot was, within uncertainties, equal to the expected difference (along the TFL) between the known isotopic compositions of olivine and aerogel.

Most of the analyzed Allende spinels were calculated to have O isotopic composition consistent with that measured for individual spinel separates distributed onto Au foil [9] (see Figure 1). The precision of the pressed-aerogel spinel measurements was similar to the spinels measured on Au foil.

We analyzed 65 particles, most $\sim$1 μm in size, in five 15μm$\times$15μm areas from the bulb of Stardust track C2052,2,74. The O isotopic composition of these particles is shown in Figure 3. Our uncertainties are dominated by counting statistics and range from $\sim$50‰ in the smaller regions to $\sim$10‰ in the larger regions (2σ).

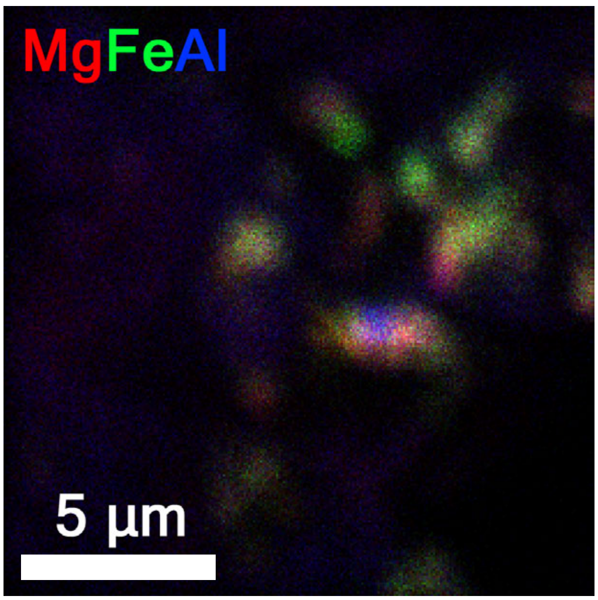

Figure 2: Scanning ion imaging map showing $^{24}Mg^{16}O^-$, $^{56}Fe^{16}O^-$, and $^{27}Al^{16}O^-$ for Map 4 from track C2052,2,74.

Discussion

We have developed a SIMS technique to measure the O isotopic composition of fine-grained Stardust cometary material still embedded in aerogel. By measuring standards of known O composition, we proved that our technique is sufficiently accurate. Cometary material is easily separated from surrounding aerogel by identifying pixels enriched in Fe, Mg, or Al. The nearby aerogel is used as the O isotope standard.

The range of O compositions seen in this fine-grained Wild 2 material span the range of all known solar system materials, from very ^{16}O-rich (mostly in Mg-rich, Fe-poor particles) to very ^{16}O-poor (in a high Fe region). The fine-grained material in this track appears to sample a much broader range of O composition than seen in larger grains in other Stardust tracks (e.g., [8, 5]).

We found no O-anomalous presolar grains so far in the bulb of track C2052,2,74. The Poisson single-sided 2σ upper limit on zero counts is 3.8 [10], which corresponds to a one-sided 2σ upper bound on the presolar grain abundance of 5.8% (3.8/65). Clearly, much more bulb material needs to be analyzed before its presolar abundance can be precisely estimated. The discovery of one presolar grain in a search of small craters on the Stardust cometary foils [11] (where dilution effects are small) corresponds to a 2σ (Poisson single-sided) upper limit of 0.8% on the presolar grain abundance.

The presence of material of varying O composition in such close proximity indicates the fine-grained component of Wild 2 is dominated by unequilibrated grains that formed in different environments. The material that deviates most from terrestrial O is located closest to the track, e.g. Map 3. Since two of the terminal particles from this track showed similar ($\sim$terrestrial) O isotopic composition in all of their components, it is likely that the bulb material and terminal particles have separate provenance—that is, the fine-grained Wild 2 material is not made up of powdered chondrules and CAIs.

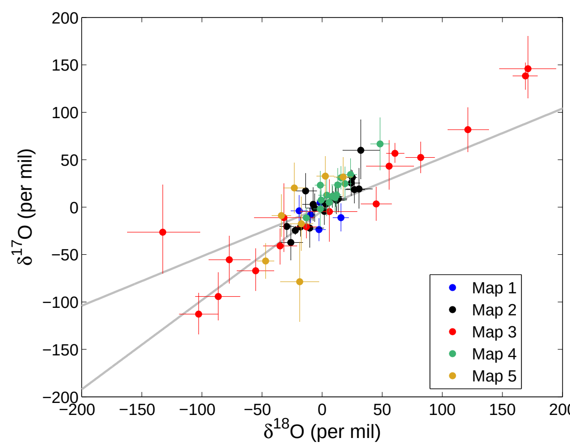

Figure 3: Oxygen 3-isotope plot showing the composition of 65 particles in five 15μm$\times$15μm areas from the bulb of Stardust track C2052,2,74. Uncertainties are 2σ.

References: [1] M. J. Burchell, et al. (2008) *Meteorit. Planet. Sci.* 43:23. [2] D. Brownlee, et al. (2012) *Meteorit. Planet. Sci.* 47:453. [3] S. B. Simon, et al. (2008) *Meteorit. Planet. Sci.* 43:1861. [4] R. C. Ogliore, et al. (2012) *ApJ* 745(2):L19. [5] D. Nakashima, et al. (2012) *Earth Planet. Sci. Lett.* 357:355. [6] J. Stodolna, et al. (2012) *Geochim. Cosmochim. Acta* 87:35. [7] A. J. Westphal, et al. (2011) *Meteorit. Planet. Sci.* 74:5274. [8] K. D. McKeegan, et al. (2006) *Science* 314:1724. [9] K. Makide, et al. (2009) *40th LPSC* #2079. [10] N. Gehrels (1986) *ApJ* 303:336. [11] J. Leitner, et al. (2010) *41st LPSC* #1607.